Probing a Dissipative Phase Transition via Dynamical Optical Hysteresis

S. R. K. Rodriguez,[1,*] W. Casteels,[2] F. Storme,[2] N. Carlon Zambon,[1] I. Sagnes,[1] L. Le Gratiet,[1] E. Galopin,[1] A. Lemaître,[1] A. Amo,[1] C. Ciuti,[2] and J. Bloch[1]

[1]*Centre de Nanosciences et de Nanotechnologies, CNRS, Université Paris-Sud, Université Paris-Saclay, C2N—Marcoussis, 91460 Marcoussis, France*

[2]*Laboratoire Matériaux et Phénomènes Quantiques, Université Paris Diderot, Sorbonne Paris Cité and CNRS, UMR 7162, 75205 Paris Cedex 13, France*

(Received 20 January 2017; revised manuscript received 30 March 2017; published 16 June 2017)

We experimentally explore the dynamical optical hysteresis of a semiconductor microcavity as a function of the sweep time. The hysteresis area exhibits a double power law decay due to the influence of fluctuations, which trigger switching between metastable states. Upon increasing the average photon number and approaching the thermodynamic limit, the double power law evolves into a single power law. This algebraic behavior characterizes a dissipative phase transition. Our findings are in good agreement with theoretical predictions for a single mode resonator influenced by quantum fluctuations, and the present experimental approach is promising for exploring critical phenomena in photonic lattices.

DOI: 10.1103/PhysRevLett.118.247402

Optical bistability—the existence of two stable states with different photon numbers for the same driving conditions—is a general feature of driven nonlinear systems described within the mean-field approximation (MFA) [1]. Beyond the MFA, a quantum treatment predicts that the steady state of a nonlinear cavity is always unique [2]. The origin of this apparent contradiction was noted by Bonifacio and Lugiato [3], and by Drummond and Walls [4]: quantum fluctuations (the lost feature in the MFA) trigger switching between states and the unique solution corresponds to a weighted average over the two metastable states. Experiments in the 1980s with two-mode lasers evidenced extremely long switching times [5], which were predicted to diverge for weak fluctuations and/or large photon numbers [6]. Already in these early works, this dramatic slowing down of the system dynamics was linked to a first order phase transition [5–7].

The physics emerging from fluctuations in nonlinear resonators is receiving renewed interest in photonics due to the emergence of nonlinear resonators such as photonic crystals [8,9], waveguides [10], superconducting microwave resonators [11,12], or optomechanical resonators [13,14]. They provide new opportunities to study quantum many-body phases [15–20], critical phenomena [19–25], and dissipative phase transitions [26]. In this context, semiconductor microcavities operating in the exciton-photon strong coupling regime enable exquisite control over photon hopping in lattices of different dimensionalities [27–29]. Their elementary excitations, namely, cavity polaritons, display strong Kerr nonlinearities via the exciton component [30–33].

Recently, it was predicted that critical exponents could be retrieved from dynamical hysteresis measurements in a single resonator [22]. When the driving power is swept at a finite speed across a bistability, the area of the hysteresis cycle is expected to close following a double power law as a function of the sweep time [22,34]. The long-time decay arises from quantum fluctuations, and presents a universal -1 exponent [22]. In the thermodynamic limit wherein the intracavity photon number tends to infinity and fluctuations are negligible, the algebraic decay of the hysteresis area is expected to evolve into a single power law [24]. This behavior characterizes a first order dissipative phase transition [24].

In this Letter, we experimentally demonstrate the algebraic decay of the dynamical optical hysteresis in semiconductor micropillars. Scanning the power up and down at decreasing speeds, we observe the progressive closure of the hysteresis cycle. The hysteresis area exhibits a temporal double power law decay with experimentally retrieved exponents in agreement with calculations including quantum fluctuations only. Probing different laser detunings and photon-photon interactions, we show that the algebraic decay evolves towards a single power law when the photon number becomes very large, i.e., when approaching the thermodynamic limit. Our results pave the way to the investigation of dissipative phase transitions in lattices of nonlinear resonators.

First, we briefly revisit the physics of a driven-dissipative single mode nonlinear cavity as illustrated in Fig. 1(a). ω_0, γ, and U represent the mode frequency, linewidth, and photon-photon interaction strength (Kerr nonlinearity) of the cavity, driven by an electromagnetic field of frequency ω and intensity I. Within the rotating-wave approximation, the Hamiltonian ($\hbar = 1$) is

$$\hat{H}(t) = \omega_0 \hat{a}^\dagger \hat{a} + \frac{U}{2} \hat{a}^\dagger \hat{a}^\dagger \hat{a} \hat{a} + \sqrt{I}(e^{-i\omega t} \hat{a}^\dagger + e^{i\omega t} \hat{a}). \quad (1)$$

The boson operator $\hat{a}$ ($\hat{a}^\dagger$) annihilates (creates) an excitation in the resonator. The dynamics is described by the Lindblad master equation for the density matrix $\hat{\rho}(t)$:

$$\frac{\partial\hat{\rho}(t)}{\partial t} = i[\hat{\rho}, \hat{H}(t)] + \frac{\gamma}{2}(2\hat{a}\,\hat{\rho}\,\hat{a}^\dagger - \hat{a}^\dagger\hat{a}\,\hat{\rho} - \hat{\rho}\hat{a}^\dagger\hat{a}). \quad (2)$$

Equation (2) can be written as $\partial_t\hat{\rho} = \hat{\mathcal{L}}\,\hat{\rho}$, where $\hat{\mathcal{L}}$ is the Liouvillian superoperator. $\hat{\mathcal{L}}$ has a complex spectrum, of which two eigenvalues λ are particularly relevant for the long-time dynamics: (i) $\lambda = 0$ corresponds to the steady state, and (ii) the nonzero eigenvalue with the real part closest to zero is the Liouvillian gap $\bar{\lambda}$.

An exact expression for the steady-state photon density predicted by Eq. (2) was found in Ref. [4]. This exact solution is shown as a gray line in Fig. 1(c), for $U/\gamma = 0.0075$ and a laser-cavity detuning $\Delta = \omega - \omega_0 = \gamma$. The MFA follows from assuming the field to be coherent with amplitude $\alpha(t) = \langle\hat{a}\rangle$. Equation (2) then reduces to $i(\partial\alpha/\partial t) = (\omega_0 - i(\gamma/2) + U|\alpha|^2)\alpha + \sqrt{I}e^{-i\omega t}$. The black line in Fig. 1(c) is the corresponding MFA calculation, displaying bistability for $31 < I/\gamma^2 < 33$. While the MFA implies a hysteresis cycle when varying the power across the bistability, the quantum solution is unique. This apparent contradiction is due to the absence of fluctuations in the MFA [3,4]. Fluctuations (quantum or classical) render the mean-field steady states metastable [36,37], and the unique steady state corresponds to their average.

The reconciliation between numerous reports of optical bistability [31,38–46] and the quantum prediction of a unique steady state [4] follows from the fact that fluctuations can take astronomical times to induce switching between metastable states. Historically, this switching time is known as the tunneling time for bistability τ_{tunn} [47–49], first-passage time [5], quantum activation time [50], or the (inverse) asymptotic decay rate [26]. We will label this characteristic time as τ_{tunn}, which is obtained by minimizing the Liouvillian gap $\bar{\lambda}$ as a function of I. $\bar{\lambda}$ is calculated numerically by diagonalizing $\hat{\mathcal{L}}$. Figure 1(d) shows τ_{tunn} as a function of Δ/γ for different U/γ. For weak interactions and/or large detunings, τ_{tunn} can vastly exceed realistic measurement times. Consequently, hysteresis measurements performed within a shorter time than τ_{tunn} lead to an apparent bistability. In this vein, Casteels and co-workers predicted how the hysteresis area should be influenced by quantum fluctuations when the scanning time across the "bistability" is commensurate with τ_{tunn} [22]. They predicted a double power law decay of the hysteresis area [22], in contrast with previous reports of a single power law decay [40].

To measure dynamic optical hysteresis, we use micropillars etched from a GaAs λ planar cavity containing one 8 nm $In_{0.04}Ga_{0.96}As$ quantum well and surrounded by two $Ga_{0.9}Al_{0.1}As/Ga_{0.05}Al_{0.95}As$ distributed Bragg reflectors with 26 and 30 pairs of layers at the top and bottom, respectively. We use rectangular micropillars where discrete states are many linewidths apart and orthogonal linearly polarized modes are nondegenerate. Thus, our configuration emulates a single mode nonlinear cavity as described by Eqs. (1) and (2). The sample is maintained at 4 K and driven by a frequency-tunable single-mode laser. We probe the lowest energy mode of the micropillars, whose linewidth ranges from 28 to 34 μeV [35]. The value of U is estimated from the energy of the confined polariton mode and its exciton fraction [35]. The laser power is modulated by an electro-optic modulator (EOM) fed by a waveform generator [see Fig. 2(a)]. The waveform contains a series of ~50 triangular ramps of variable time duration. The transmission through the cavity is measured with a photodiode connected to an oscilloscope. The scanning times t_s (the time it takes to ramp the power from the lowest to the highest value) span the 0.8–50 kHz range. As shown in the Supplemental Material, laser shot noise is the only noise source within this frequency range and we exclude additional fluctuations from our observations [35].

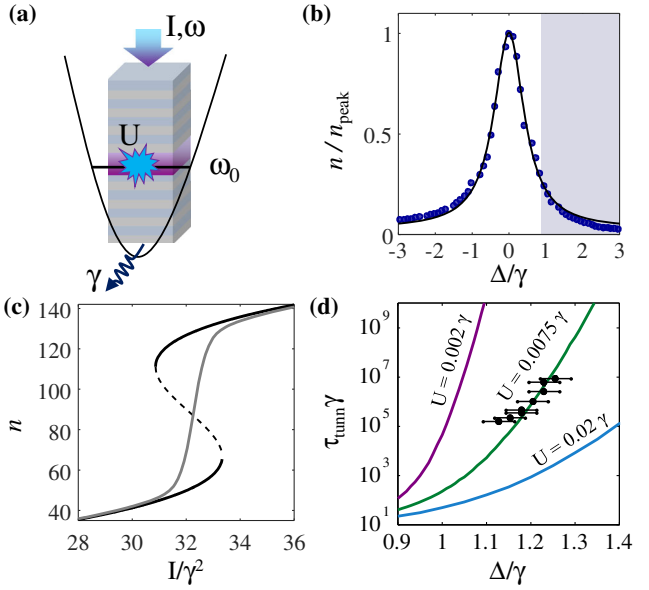

FIG. 1. (a) Sketch of a microcavity with mode frequency ω_0, loss rate γ, photon-photon interactions of strength U, driven by an electromagnetic field of intensity I and frequency ω. (b) Normalized photon density in a semiconductor microcavity under weak driving. Experimental data points for the sample studied in Figs. 2, 3, and 4 are fitted with a Lorentzian line shape. The shaded area indicates the mean-field bistable regime $\Delta \equiv \omega - \omega_0 > \sqrt{3}\gamma/2$ for $U > 0$. (c) Mean-field (black curves) and quantum (gray curves) solutions for a cavity with $U = 0.0075\ \gamma$ probed at $\Delta = \gamma$. In the mean-field solution, the solid and dashed curves are stable and unstable states, respectively. (d) Tunneling time τ_{tunn} between the two mean-field states. Data points are residence time measurements [35].

We are interested in the hysteresis area,

$$A = \int_{P_{\text{min}}}^{P_{\text{max}}} |n_\downarrow(P) - n_\uparrow(P)|dP, \quad (3)$$

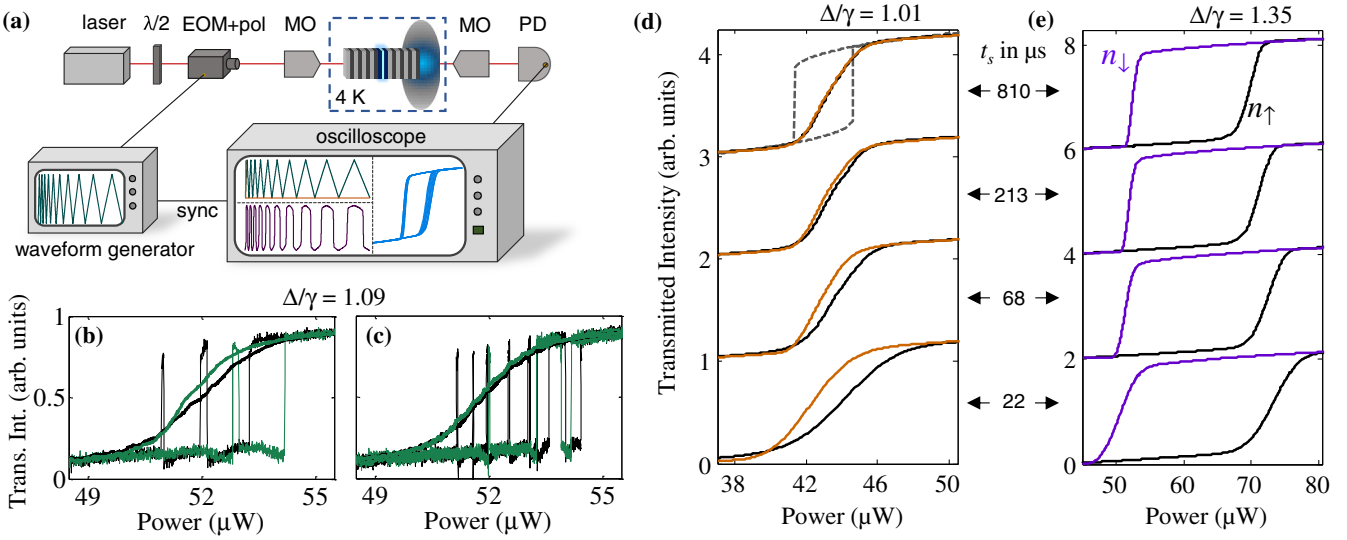

FIG. 2. (a) Experimental setup: $\lambda/2$, MO, PD, and EOM + pol, stand for half-wave plate, microscope objective, photodiode, and electro-optic modulator with a polarizer, respectively. The green (purple) traces in the waveform generator and in the oscilloscope are measurements of the incident (transmitted) signals. The hysteresis cycles in the oscilloscope are the transmitted versus the incident signal, overlaid for various scanning times. The colored and black lines in (b)–(e) represent the transmission when the power is ramped down and up, respectively. (b) and (c) show single shot (thin lines) and averages over 1000 realizations (thick lines) of dynamic hysteresis. The scanning time is $t_s = 0.11$ ms in (b), and $t_s = 0.43$ ms in (c). (d) and (e) show dynamic hysteresis averaged over 1500 realizations for values of t_s indicated between the two panels. The dashed line in (d) is the mean-field calculation corresponding to the experiment.

as a function of t_s. $n_\downarrow(P)$ and $n_\uparrow(P)$ represent the cavity transmission when the power is ramped down and up, respectively. $P_{\min}$ and $P_{\max}$ are powers below and above the hysteresis range. In the absence of fluctuations, A saturates to a finite value (the mean-field static hysteresis area) for $t_s \to \infty$ [40]. However, unavoidable quantum fluctuations induce switchings between the mean-field "bistable" states. Consequently, the hysteresis area averaged over many realizations, $A_{\rm av}$, is expected to close in proportion to the number of switching events such that $\lim_{t_s\to\infty} A_{\rm av} = 0$.

In Figs. 2(b) and 2(c) we compare single-shot (thin lines) and averaged (thick lines, 1000 realizations) transmission measurements for a micropillar of lateral dimensions 4×2 μm^2 probed at $\Delta/\gamma = 1.09$. The single-shot measurements in Fig. 2(c) display more switchings than in Fig. 2(b) because the sweep is slower in Fig. 2(c). Consequently, $A_{\rm av}$ is reduced in Fig. 2(c).

Figure 2(d) shows hysteresis measurements (averaged over 1500 realizations) for $\Delta/\gamma = 1.01$ and different values of t_s. $A_{\rm av}$ closes for increasing t_s. For the slowest sweep, the measured cycle strongly deviates from the mean-field prediction (dashed lines) and resembles the exact quantum prediction in Fig. 1(c). In contrast, for larger Δ/γ, $\tau_{\rm tunn} \gg t_s$ and $A_{\rm av}$ changes marginally [see Fig. 2(e)].

The behavior of $A_{\rm av}$ not only depends on t_s, but also on the scanned power range $P_s \equiv P_{\max} - P_{\min}$. The ratio t_s/P_s gives an effective (inverse) sweep speed. In Fig. 3(a) we plot $A_{\rm av}$ as a function of t_s/P_s for six different Δ/γ. For small Δ/γ we observe two power laws indicated by the gray and blue lines in Fig. 3(a). The blue lines correspond to a power law with a -1 exponent, as expected when $\tau_{\rm tunn} < t_s$ [22]. For increasing Δ/γ, the average photon number in the bistability increases and fluctuations become relatively weaker. This shifts the onset of the -1 power law to times far beyond our observation window.

Calculating the dynamics behind the results in Fig. 3(a) requires a time evolution up to 10^8 times the polariton lifetime (21 ps), a temporal resolution below the polariton lifetime, and a dimensionality of the Hilbert space of $\sim 10^3$. To circumvent this difficulty, Ref. [22] introduced a method based on a scaling analysis in the spirit of the Kibble-Zurek mechanism for dynamic phase transitions [51]. The key idea is that a power sweep at a finite rate across the bistability involves a nonadiabatic response of the system, resulting in hysteresis. The nonadiabatic intensity range δI is determined by comparing the sweep time scale τ_S with the system reaction time τ_R (see Fig. 3(b) inset and Ref. [35]), obtained by diagonalizing $\hat{\mathcal{L}}$. Similar to $A_{\rm av}$, δI exhibits a double power law as a function of the sweep rate [22].

Figure 3(b) shows calculations of δI for the same values of Δ/γ considered in experiments. The lines in Fig. 3(b) are power laws with exponents obtained from fits to the measurements in Fig. 3(a). Excellent agreement between experiments and theory is demonstrated by the fact that we do not fit the exponent of the power laws in Fig. 3(b) to the calculations of δI. We only adjusted the value of U/γ within the experimental uncertainty. We take $U/\gamma = 7.5 \times 10^{-3}$, whereas the experimental estimate [35] is $U/\gamma = 2 \times 10^{-3}{}^{+8\times10^{-3}}_{-1.6\times10^{-3}}$. Overall, Fig. 3 shows that as Δ/γ

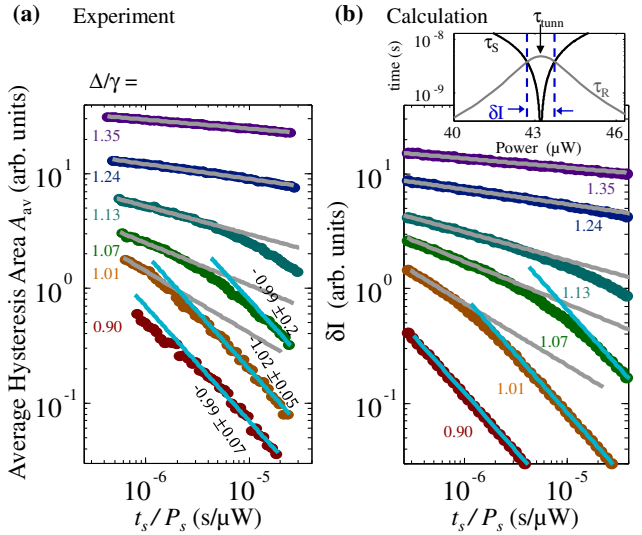

FIG. 3. (a) Measured average hysteresis area A_{av} as a function of t_s/P_s, with P_s the scanned power range. Different colors correspond to different values of Δ/γ. The gray and blue lines are power law fits. The exponents fitted in the regime influenced by fluctuations (blue lines) are shown with 2σ confidence intervals. (b) Calculations of the nonadiabatic range δI of the driving intensity using the scaling analysis described in the text. All power laws in (b) have the same exponents retrieved from the fits in (a). The inset in (b) shows the system reaction time τ_R in gray, and the sweep time scale τ_S in black, for $U = 0.0075\,\gamma$, $\Delta = 1.01\,\gamma$, and $t_s/P_s = 10^{-6}$ s/μW. The dashed lines indicate the nonadiabatic range δI. The conversion of the theoretical intensity units to the experimental power units is described in the Supplemental Material [35].

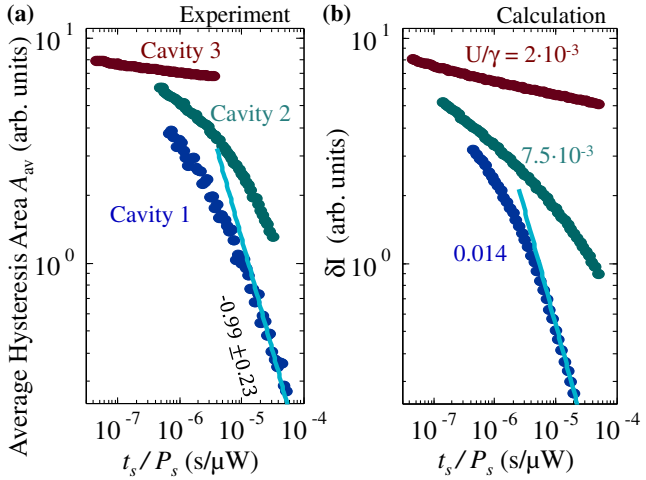

FIG. 4. (a) Measured average hysteresis area A_{av} for cavities with different U/γ (decreasing from cavity 1 to cavity 3) and approximately equal Δ/γ. Cavity 2 is the same one studied in Figs. 1–3. (b) Calculations of δI as explained in Fig. 3. For the highest and lowest curves $\Delta/\gamma = 1.15 \pm 0.1$, while for the middle curve $\Delta/\gamma = 1.13 \pm 0.1$, in experiments and calculations. In (a), data for cavity 3 was divided by 80. In (b), data for the smallest U/γ was divided by 4, and data for the largest U/γ was multiplied by 2. These multiplications (for improving visibility) only shift the curves vertically and do not change the exponent.

decreases and the photon number in the bistability decreases, the hysteresis area evolves from a single to a double power law decay. The power law at large Δ/γ or small t_s is also present in the absence of fluctuations [40]. This generic feature of classical nonlinear systems is due to a shift of the limit point where the system jumps between branches for increasing drive speed [40,52]. The power law at large t_s is due to the influence of fluctuations, which could be classical (e.g., thermal [34]) or quantum. To verify that the -1 power law we observe is due to quantum fluctuations, we compare the characteristic time scale of the stochastic jumps leading to the closure of A_{av} [see Figs. 2(b) and 2(c)] with τ_{tunn}. In particular, we measured the residence time of the system in the metastable states [35]. The results, presented in Fig. 1(d), are in good agreement with calculations including quantum fluctuations only. Thermal fluctuations and nonlinear losses (e.g., collisional broadening [53]), neglected in the master equation used to calculate τ_{tunn}, are unnecessary to reproduce our experiments.

A thermodynamic limit can be defined for a single resonator by letting the photon number $N \to \infty$ and $U \to 0$ while keeping UN constant [24]. This limit can be explored probing cavities with different values of U/γ at a fixed laser-cavity detuning Δ/γ. Experimentally, we vary U/γ by selecting micropillars with different lateral dimensions. A reduced cross-sectional area of the micropillar blueshifts the energy of the confined polariton modes and increases their exciton fraction, thereby increasing U/γ [35]. Figure 4(a) shows measurements of A_{av} for three cavities probed at $\Delta/\gamma = 1.15 \pm 0.1$. For cavity 1 with the strongest interaction strength, A_{av} displays a double power law with the -1 exponent at large t_s/P_s. As U/γ decreases, the time at which the power law with the -1 exponent sets in increases. For cavity 3 with the weakest interaction strength, A_{av} depends marginally on t_s/P_s and the data follow a single power law. These observations are consistent with the dramatic dependence of τ_{tunn} on U/γ plotted in Fig. 1(d).

Figure 4(b) shows calculations based on the scaling analysis previously described, in good agreement with the measurements in Fig. 4(a). Details about the values of U/γ used in the calculations are discussed in the Supplemental Material [35]. Overall, Fig. 4 demonstrates that as $U \to 0$ and the average photon number in the bistability increases, the hysteresis area evolves towards a single power-law decay. This is the signature of a system approaching the thermodynamic limit of high photon numbers [24].

To summarize, we showed a temporal double power law decay of the hysteresis area of single nonlinear resonators. The power laws observed for large scanning times exhibit an exponent equal to -1 for different laser-cavity detunings and nonlinearities, as expected due to the influence of quantum fluctuations. In the thermodynamic limit of large photon

numbers, mean-field bistability is unaffected by fluctuations: the hysteresis area exhibits a single power law decay associated with a dissipative phase transition. These results open the way to the exploration of dissipative phase transitions in lattices of micropillars, where photon hopping can give rise to intriguing behavior. For instance, a square lattice of bistable resonators has been mapped to an equilibrium Ising model with an effective temperature given by the losses [25]. The question remains open regarding phase transitions in more elaborate lattices with intricate topologies [54], with spin-orbit coupling [55], or with quasicrystalline structure [56] in which thermodynamic properties reflect their noninteger dimensions [57,58].

This work was supported by the Marie Curie individual fellowship PINQUAR (Project No. 657042), the French National Research Agency (ANR) program Labex NanoSaclay via the projects Qeage (ANR- 11-IDEX-0003-02), ICQOQS (ANR-10-LABX-0035), and Quantum Fluids of Light (ANR-16-CE30-0021), the French RENATECH network, the ERC grant Honeypol and the EU-FET Proactiv grant AQUS (Project No. 640800). W. C., F. S., and C. C. acknowledge support from European Research Council (ERC) (via the Consolidator Grant "CORPHO" No. 616233).

*said.rodriguez@u-psud.fr

[1] H. M. Gibbs, *Optical Bistability: Controlling Light with Light*, Quantum Electronics Series (Academic Press, New York, 1985).
[2] D. F. Walls and G. J. Milburn, *Quantum Optics* (Springer, Berlin, Heidelberg, 2008).
[3] R. Bonifacio and L. A. Lugiato, Photon Statistics and Spectrum of Transmitted Light in Optical Bistability, Phys. Rev. Lett. **40**, 1023 (1978).
[4] P. D. Drummond and D. F. Walls, Quantum theory of optical bistability. I. Nonlinear polarisability model, J. Phys. A **13**, 725 (1980).
[5] R. Roy, R. Short, J. Durnin, and L. Mandel, First-Passage-Time Distributions under the Influence of Quantum Fluctuations in a Laser, Phys. Rev. Lett. **45**, 1486 (1980).
[6] F. T. Hioe and S. Singh, Correlations, transients, bistability, and phase-transition analogy in two-mode lasers, Phys. Rev. A **24**, 2050 (1981).
[7] P. Lett, W. Christian, S. Singh, and L. Mandel, Macroscopic Quantum Fluctuations and First-Order Phase Transition in a Laser, Phys. Rev. Lett. **47**, 1892 (1981).
[8] A. Majumdar, A. Rundquist, M. Bajcsy, V. D. Dasika, S. R. Bank, and J. Vučković, Design and analysis of photonic crystal coupled cavity arrays for quantum simulation, Phys. Rev. B **86**, 195312 (2012).
[9] P. Hamel, S. Haddadi, F. Raineri, P. Monnier, G. Beaudoin, I. Sagnes, A. Levenson, and A. M. Yacomotti, Spontaneous mirror-symmetry breaking in coupled photonic-crystal nanolasers, Nat. Photonics **9**, 311 (2015).
[10] J. W Fleischer, M. Segev, N. K. Efremidis, and D. N. Christodoulides, Observation of two-dimensional discrete solitons in optically induced nonlinear photonic lattices, Nature (London) **422**, 147 (2003).
[11] R. Vijay, M. H. Devoret, and I. Siddiqi, The Josephson bifurcation amplifier, Rev. Sci. Instrum. **80**, 111101 (2009).
[12] D. L. Underwood, W. E. Shanks, Jens Koch, and A. A. Houck, Low-disorder microwave cavity lattices for quantum simulation with photons, Phys. Rev. A **86**, 023837 (2012).
[13] M. Eichenfield, J. Chan, R. M. Camacho, K. J. Vahala, and O. Painter, Optomechanical crystals, Nature (London) **462**, 78 (2009).
[14] E. Gil-Santos, M. Labousse, C. Baker, A. Goetschy, W. Hease, C. Gomez, A. Lemaître, G. Leo, C. Ciuti, and I. Favero, Light-Mediated Cascaded Locking of Multiple Nano-Optomechanical Oscillators, Phys. Rev. Lett. **118**, 063605 (2017).
[15] M. J. Hartmann, F. G. S. L. Brandao, and M. B. Plenio, Strongly interacting polaritons in coupled arrays of cavities, Nat. Phys. **2**, 849 (2006).
[16] A. D. Greentree, C. Tahan, J. H. Cole, and L. C. L. Hollenberg, Quantum phase transitions of light, Nat. Phys. **2**, 856 (2006).
[17] D. G. Angelakis, M. F. Santos, and S. Bose, Photon-blockade-induced Mott transitions and *XY* spin models in coupled cavity arrays, Phys. Rev. A **76**, 031805 (2007).
[18] A. Le Boité, G. Orso, and C. Ciuti, Steady-State Phases and Tunneling-Induced Instabilities in the Driven Dissipative Bose-Hubbard Model, Phys. Rev. Lett. **110**, 233601 (2013).
[19] R. M. Wilson, K. W. Mahmud, A. Hu, A. V. Gorshkov, M. Hafezi, and M. Foss-Feig, Collective phases of strongly interacting cavity photons, Phys. Rev. A **94**, 033801 (2016).
[20] M. Biondi, G. Blatter, H. E. Türeci, and S. Schmidt, Nonequilibrium phase diagram of the driven-dissipative photonic lattice, arXiv:1611.00697.
[21] H. J. Carmichael, Breakdown of Photon Blockade: A Dissipative Quantum Phase Transition in Zero Dimensions, Phys. Rev. X **5**, 031028 (2015).
[22] W. Casteels, F. Storme, A. Le Boité, and C. Ciuti, Power laws in the dynamic hysteresis of quantum nonlinear photonic resonators, Phys. Rev. A **93**, 033824 (2016).
[23] J. J. Mendoza-Arenas, S. R. Clark, S. Felicetti, G. Romero, E. Solano, D. G. Angelakis, and D. Jaksch, Beyond mean-field bistability in driven-dissipative lattices: Bunching-antibunching transition and quantum simulation, Phys. Rev. A **93**, 023821 (2016).
[24] W. Casteels, R. Fazio, and C. Ciuti, Critical dynamical properties of a first-order dissipative phase transition, Phys. Rev. A **95**, 012128 (2017).
[25] M. Foss-Feig, P. Niroula, J. T. Young, M. Hafezi, A. V. Gorshkov, R. M. Wilson, and M. F. Maghrebi, Emergent equilibrium in many-body optical bistability, Phys. Rev. A **95**, 043826 (2017).
[26] E. M. Kessler, G. Giedke, A. Imamoglu, S. F. Yelin, M. D. Lukin, and J. I. Cirac, Dissipative phase transition in a central spin system, Phys. Rev. A **86**, 012116 (2012).
[27] I. Carusotto and C. Ciuti, Quantum fluids of light, Rev. Mod. Phys. **85**, 299 (2013).
[28] N. Y. Kim, K. Kusudo, C. Wu, N. Masumoto, A. Löffler, S. Höfling, N. Kumada, L. Worschech, A. Forchel, and Y. Yamamoto, Dynamical d-wave condensation of

exciton-polaritons in a two-dimensional square-lattice potential, Nat. Phys. **7**, 681 (2011).
[29] F. Baboux, L. Ge, T. Jacqmin, M. Biondi, E. Galopin, A. Lemaître, L. Le Gratiet, I. Sagnes, S. Schmidt, H. E. Türeci, A. Amo, and J. Bloch, Bosonic Condensation and Disorder-Induced Localization in a Flat Band, Phys. Rev. Lett. **116**, 066402 (2016).
[30] A. Amo, J. Lefrère, S. Pigeon, C. Adrados, C. Ciuti, I. Carusotto, R. Houdré, E. Giacobino, and A. Bramati, Superfluidity of polaritons in semiconductor microcavities, Nat. Phys. **5**, 805 (2009).
[31] A. Baas, J. Ph. Karr, H. Eleuch, and E. Giacobino, Optical bistability in semiconductor microcavities, Phys. Rev. A **69**, 023809 (2004).
[32] T. K. Paraïso, M. Wouters, Y. Léger, F. Morier-Genoud, and B. Deveaud-Plédran, Multistability of a coherent spin ensemble in a semiconductor microcavity, Nat. Mater. **9**, 655 (2010).
[33] S. R. K. Rodriguez, A. Amo, I. Sagnes, L. Le Gratiet, E. Galopin, A. Lemaître, and J. Bloch, Interaction-induced hopping phase in driven-dissipative coupled photonic microcavities, Nat. Commun. **7**, 11887 (2016).
[34] C. N. Luse and A. Zangwill, Discontinuous scaling of hysteresis losses, Phys. Rev. E **50**, 224 (1994).
[35] See Supplemental Material at http://link.aps.org/supplemental/10.1103/PhysRevLett.118.247402 for details of the sample, setup characterization, noise measurements, residence time measurements, mean-field calculations, scaling analysis, estimates of the polariton-polariton interaction constant in different micropillars, and comparison between measurements and calculations.
[36] J. Kerckhoff, M. A. Armen, and H. Mabuchi, Remnants of semiclassical bistability in the few-photon regime of cavity QED, Opt. Express **19**, 24468 (2011).
[37] H. Abbaspour, G. Sallen, S. Trebaol, F. Morier-Genoud, M. T. Portella-Oberli, and B. Deveaud, Effect of a noisy driving field on a bistable polariton system, Phys. Rev. B **92**, 165303 (2015).
[38] H. M. Gibbs, S. L. McCall, and T. N. C. Venkatesan, Differential Gain and Bistability using a Sodium-Filled Fabry-Perot Interferometer, Phys. Rev. Lett. **36**, 1135 (1976).
[39] A. Dorsel, J. D. McCullen, P. Meystre, E. Vignes, and H. Walther, Optical Bistability and Mirror Confinement Induced by Radiation Pressure, Phys. Rev. Lett. **51**, 1550 (1983).
[40] P. Jung, G. Gray, R. Roy, and P. Mandel, Scaling Law for Dynamical Hysteresis, Phys. Rev. Lett. **65**, 1873 (1990).
[41] G. Rempe, R. J. Thompson, R. J. Brecha, W. D. Lee, and H. J. Kimble, Optical Bistability and Photon Statistics in Cavity Quantum Electrodynamics, Phys. Rev. Lett. **67**, 1727 (1991).
[42] L. Collot, V. Lefvre-Seguin, M. Brune, J. M. Raimond, and S. Haroche, Very high-Q whispering-gallery mode resonances observed on fused silica microspheres, Europhys. Lett. **23**, 327 (1993).
[43] V. R. Almeida and M. Lipson, Optical bistability on a silicon chip, Opt. Lett. **29**, 2387 (2004).
[44] M. Notomi, A. Shinya, S. Mitsugi, G. Kira, E. Kuramochi, and T. Tanabe, Optical bistable switching action of si high-q photonic-crystal nanocavities, Opt. Express **13**, 2678 (2005).
[45] G. A. Wurtz, R. Pollard, and A. V. Zayats, Optical Bistability in Nonlinear Surface-Plasmon Polaritonic Crystals, Phys. Rev. Lett. **97**, 057402 (2006).
[46] T. Boulier *et al.*, Polariton-generated intensity squeezing in semiconductor micropillars, Nat. Commun. **5**, 3260 (2014).
[47] H. Risken, C. Savage, F. Haake, and D. F. Walls, Quantum tunneling in dispersive optical bistability, Phys. Rev. A **35**, 1729 (1987).
[48] K. Vogel and H. Risken, Quantum-tunneling rates and stationary solutions in dispersive optical bistability, Phys. Rev. A **38**, 2409 (1988).
[49] H. Risken and K. Vogel, Quantum tunneling rates in dispersive optical bistability for low cavity damping, Phys. Rev. A **38**, 1349 (1988).
[50] M. Dykman, *Fluctuating Nonlinear Oscillators: From Nanomechanics to Quantum Superconducting Circuits* (Oxford University Press, Oxford, 2012).
[51] J. Dziarmaga, Dynamics of a quantum phase transition and relaxation to a steady state, Adv. Phys. **59**, 1063 (2010).
[52] P. Mandel and T. Erneux, Dynamics of nascent hysteresis in optical bistability, Opt. Commun. **44**, 55 (1982).
[53] C. Ciuti, V. Savona, C. Piermarocchi, A. Quattropani, and P. Schwendimann, Threshold behavior in the collision broadening of microcavity polaritons, Phys. Rev. B **58**, R10123 (1998).
[54] T. Jacqmin, I. Carusotto, I. Sagnes, M. Abbarchi, D. D. Solnyshkov, G. Malpuech, E. Galopin, A. Lemaître, J. Bloch, and A. Amo, Direct Observation of Dirac Cones and a Flatband in a Honeycomb Lattice for Polaritons, Phys. Rev. Lett. **112**, 116402 (2014).
[55] V. G. Sala, D. D. Solnyshkov, I. Carusotto, T. Jacqmin, A. Lemaître, H. Terças, A. Nalitov, M. Abbarchi, E. Galopin, I. Sagnes, J. Bloch, G. Malpuech, and A. Amo, Spin-Orbit Coupling for Photons and Polaritons in Microstructures, Phys. Rev. X **5**, 011034 (2015).
[56] D. Tanese, E. Gurevich, F. Baboux, T. Jacqmin, A. Lemaître, E. Galopin, I. Sagnes, A. Amo, J. Bloch, and E. Akkermans, Fractal Energy Spectrum of a Polariton Gas in a Fibonacci Quasiperiodic Potential, Phys. Rev. Lett. **112**, 146404 (2014).
[57] E. Akkermans, G. V. Dunne, and A. Teplyaev, Physical consequences of complex dimensions of fractals, Europhys. Lett. **88**, 40007 (2009).
[58] E. Akkermans, G. V. Dunne, and A. Teplyaev, Thermodynamics of Photons on Fractals, Phys. Rev. Lett. **105**, 230407 (2010).